*Tribology Letters, Vol. 21, No. 3, March 2006 (© 2006)*
DOI: 10.1007/s11249-006-9030-y


# Measurement of the mechanical properties of thin films mechanically confined within contacts

E. Gacoin[a], C. Fretigny[a], A. Chateauminois[a,*], A. Perriot[b] and E. Barthel[b]

[a]*Laboratoire de Physico-Chimie des Polymères et des Milieux Dispersés, UMR CNRS 7615, Ecole de Physique et Chimie Industrielles (ESPCI), 10 rue Vauquelin, Paris Cedex 05 75231, France*
[b]*Laboratoire CNRS/Saint-Gobain, Surface du Verre et Interfaces, 39, quai Lucien Lefranc, BP 135, Aubervilliers Cedex F-93303, France*

Received 22 November 2005; accepted 18 January 2006; published online 25 April 2006

This study addresses the problem of the measurement of the mechanical properties of thin films using contact mechanics methods. In a first stage, an analytical contact model recently developed by Perriot and Barthel [A. Perriot and Barthel, E. J. Mat. Res, 2004. 19(2): 600–608] is used to derive a first order approximation within the limits of confined geometries. Together with indentation experiments using polymer films on elastic substrates, this approach demonstrates the essentially oedometric nature of the coating's response, provided it is not to close to incompressibility. In a second stage, an extension of this approximate description to lateral contact loading allowed to relate the contact stiffness to the shear modulus of the film. This approach was successfully applied to the determination of the viscoelastic modulus of an acrylate polymer film in the glass transition zone of the film, with an emphasis on its sensitivity to hydrostatic pressure. This study suggests that lateral contact experiments are more appropriate than indentation ones for the measurement of film properties close to incompressibility.

**KEY WORDS:** mechanical confinement, thin films, indentation, lateral contact stiffness, viscoelastic properties

**Nomenclature**

| | |
|---|---|
| $a$ | Radius of the contact area. |
| $E_0$, $E_1$ | Young's moduli of the substrate and the film, respectively. |
| $E_0^*$, $E_1^*$ | Reduced moduli of the substrate and the film, respectively. |
| $\tilde{E}_1$ | Oedometric modulus of the film. |
| $G_0$, $G_1$ | Coulomb's moduli of the substrate and the film, respectively. |
| $G_1'$ | Storage modulus of the film. |
| $k_c$ | Lateral stiffness of the coated contact. |
| $k_f$ | Shear stiffness of the film within the contact. |
| $k_s$ | Lateral contact stiffness of the sphere-on-flat contact without a film. |
| $P$ | Applied normal contact load. |
| $\bar{P}$ | Reduced contact load defined as $\bar{P} = 3PR/4E_1^* a^3$ |
| $R$ | Radius of the glass lens. |
| $t$ | Film thickness. |
| $u_1$, $u_0$ | Vertical displacement of the surface of the film and of the film/substrate interface, respectively. |
| $\sigma_1$, $\sigma_0$ | Normal stress at the surface of the film and at the film substrate/interface, respectively. |
| $\nu_0$, $\nu_1$ | Poisson's ratio of the substrate and the layer respectively. |

## 1. Introduction

The increasing use of layered and multilayered systems has motivated a growing interest for the measurement of the mechanical properties of thin films. Among various techniques, contact experiments such as nano-indentation have emerged as a promising route. However, the analysis of nano-indentation data usually relies on contact mechanics models (such as the popular Oliver and Pharr model [1]), which were developed for isotropic and homogeneous elastic solids. In the case of layered systems, the use of these approaches yields a "composite" modulus, which incorporates the depth-dependent contributions of the film and the substrate. In order to extract the film modulus from this measured composite modulus, various empirical and semi-empirical models have been proposed on the basis of experimental data or finite element simulations. Most of them express the composite modulus as a linear or non linear combination of the modulus of the substrate and of the film [2–6]. Alternatively, analytical approaches have also been developed by Gao *et al.* [7] in order to derive approximate expressions for the contact compliance within the limits of moduli ratios not exceeding a factor of two.

These approaches have been successfully applied to nano-indentation experiments where the ratio of the contact radius to the film thickness remains close to unity, i.e. for contact conditions, which are characterized by a low geometrical confinement. However, nano-indentation experiments carried out using very thin

*To whom correspondence should be addressed.
E-mail: antoine.chateauminois@espci.fr

films can sometimes give rise to substantial levels of confinement, even when they are carried out using sharp indenters. This geometrical confinement is especially characterized by a high level of hydrostatic pressure, which some materials such as polymers are known to be sensitive to. As a matter of fact, some recent nano-indentation experiments using polymer coatings and pyramidal or conical indenters show that, when the indentation depth becomes of the order of magnitude of the film thickness, the above mentioned indentation models can provide erroneous [8] or unexpectedly high values of the layer Young's modulus [9]. The question thus arises to establish whether such results are the consequence of some limitations of the models under confined contacts situations or they are hydrostatic pressure effects, as it is argued in references [8–11].

The objective of this paper is to investigate these issues from a discussion of theoretical and experimental results. In addition to indentation loading, the potential of lateral contact experiments for the measurement of the mechanical properties of confined films will be considered. The analysis is restricted to the case of a soft layer on a more rigid substrate. In a first stage, the analytical elastic contact model recently derived by Perriot and Barthel [12] is used as a basis to develop a first order approximation of the indentation response of confined coatings. This approximation shows the essentially oedometric nature of the film compressive response. It is also supported by indentation experiments on glassy polymer films within contact between an elastic substrate and an elastic sphere. In a second stage, this analysis of the contact deformation modes is extended to lateral contact loading. This allows deriving an approximate expression, which relates the measured contact stiffness to the shear modulus of the layer. This expression indicates that lateral contact experiments should be much more insensitive than indentation ones to the incompressibility of the layer. As an example, the shear modulus of a polymer film is measured by lateral methods in the glass transition zone, i.e. in conditions close to incompressibility.

## 2. Indentation response of confined layered systems

### 2.1. Formulation of the approximate contact model

Let us consider the system depicted in figure 1(a), which consists of a coated elastic substrate in contact with a rigid sphere. $E_i$ and $\nu_i$ denote the Young's modulus and the Poisson's ratio of the layer ($i=1$) and of the substrate ($i=0$). Within the frame of this study, only geometrically confined contact situations will be considered, which means that the ratio of the contact radius, $a$, to the film thickness, $t$, will be kept much greater than unity. In addition, the discussion will be restricted to case of a soft layer on a more rigid substrate, i.e. $E_0 \gg E_1$.

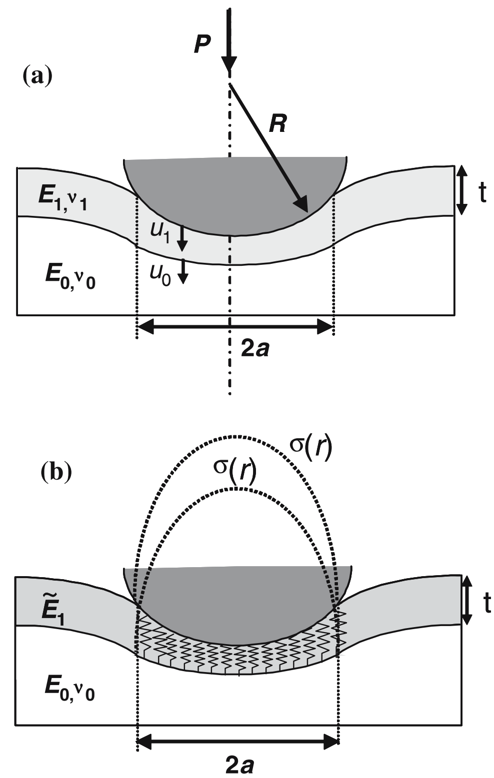


Figure 1. Schematic description of the elastic indentation of a coated substrate by a rigid sphere. (a) Actual contact configuration. The layer is assumed to be perfectly bound to the substrate and the contact interface is frictionless. $E_i$ and $\nu_i$ are the Young's modulus and the Poisson's ratio of the substrate ($i=0$) and the layer ($i=1$). (b) Oedometric approximation within the limits of confined contact geometries. The layer is considered to behave in compression as a mattress of elastic stiffnesses set in parallel. The effective compression modulus of the layer is the oedometric modulus of the material, $\tilde{E}_1$. The applied normal stress, $\sigma$, is assumed to be integrally transmitted to the film/substrate interface over a constant contact area of radius, $a$.

The expression derived independently by Li and Chou [13] and by Nogi and Kato [14] for the Green function for a layered substrate has been taken as a starting point for the development of an approximate contact model. Within the framework of linear elasticity, these authors have derived an expression relating the Hankel transforms of the normal displacement, $u_1(r)$, to that of the applied normal stress, $\sigma(r)$, at the surface of the elastic layer:

$$\bar{u}_1(\xi) = \frac{2}{E_1^*}\frac{X(\xi)}{\xi}\bar{\sigma}(\xi) \qquad (1)$$

$E_1^*$ being the reduced modulus of the layer defined as $E_1/(1-\nu_1^2)$ and $X(\xi)$ is defined as:

$$X(\xi) = \frac{1 + 4b\xi t e^{-2\xi t} - abe^{-4\xi t}}{1 - \left(a + b + 4b(\xi t)^2\right)e^{-2\xi t} + abe^{-4\xi t}}$$

$$a = \frac{\alpha\gamma_0 - \gamma_1}{1 + \alpha\gamma_0}, b = \frac{\alpha - 1}{\alpha + \gamma_1}, \alpha = \frac{G_1}{G_0},$$

$$\gamma_1 = 3 - 4\nu_1, \gamma_0 = 3 - 4\nu_0 \qquad (2)$$

where $G_0$ and $G_1$ denote the shear moduli of the substrate and the layer, respectively. In equation (1), the quantities in the form of $\bar{q}(\xi)$ correspond to the 0th-order Hankel transform of the function $q(r)$ defined as:

$$\bar{q}(\xi) = \int_0^\infty drrJ_0(\xi r)q(r)$$

with $J_0(x)$ the 0th-order Bessel function of the first kind.

In the above expressions, the Hankel transform of the fields are equivalent to their two-dimensional Fourier transforms, as they are radially symmetric. Then, as the normal stress is zero out of the contact area, it is expected that its Hankel transform varies at the scale of $1/a$. On another hand, we can deduce from its expression that $X(\xi)$ varies at the scale of $1/t$. Thus, in the case of confined contacts, i.e. $t \ll a$, it is presumably sufficient to consider a first order expansion of $X(\xi)$ in order to invert equation (1). Moreover, assuming that the layer modulus is much lower than the substrate one, the expansion can be written:

$$X(\xi) \approx \frac{2}{E_0^*} + \frac{1}{\tilde{E}_1}\xi t \tag{3}$$

where the effective modulus, $\tilde{E}_1$, can be expressed in the following form after some calculations:

$$\tilde{E}_1 = E_1 \frac{(1-\nu_1)}{[(1-2\nu_1)(1+\nu_1)]}, \quad E_1 \ll E_0 \tag{4}$$

It can easily be recognized that $\tilde{E}_1$ is in fact the so-called oedometric or longitudinal bulk modulus [15,16] of the layer, which corresponds to the elastic response of the constrained material under compression or extension, deformation in the lateral dimension being prevented. This finding is physically consistent with the expected deformation mode of a layer confined within a contact. Accordingly, equation (1) can be rewritten as:

$$\bar{u}_1 \approx \frac{2}{E_0^*}\frac{1}{\xi}\bar{\sigma} + \frac{t}{\tilde{E}_1}\bar{\sigma} \tag{5}$$

If the effects of shear are neglected, the deformation of the film/substrate interface must obey the following relationship:

$$\bar{u}_1 = \frac{2}{E_0^*}\frac{1}{\xi}\bar{\sigma}_0 \tag{6}$$

where $\bar{\sigma}_0$ is the Hankel transform of the normal stress at the interface. Using equations (6) and (7) one can write:

$$\bar{u}_1 - \bar{u}_0 = \frac{t}{\tilde{E}_1}\bar{\sigma} + \frac{2}{E_0^*}\frac{1}{\xi}(\bar{\sigma} - \bar{\sigma}_0) \tag{7}$$

Under confined conditions, it can be assumed that, within the coating, stresses do not expand significantly outside the contact zone. In other words, the normal stress, $\sigma$, applied to the surface of the layer should be integrally transmitted to the substrate over a constant circular area of radius, $a$. $\bar{\sigma}$ and $\bar{\sigma}_0$ can therefore be equated, giving:

$$\bar{u}_1 - \bar{u}_0 = \frac{t}{\tilde{E}_1}\bar{\sigma} \tag{8}$$

which can be expressed in the real space as:

$$u_1 - u_0 = \frac{t}{\tilde{E}_1}\sigma \tag{9}$$

From equation (9), it turns out that, at any location within the contact, the compression of the film is proportional to the applied normal stress. It can therefore be considered that the confined layer acts mechanically as a “mattress” of individual springs, each of them having the same compliance, $t/\tilde{E}_1$ (figure 1(b)). In passing, it can be noted that such a picture of the compressive response of the coating is very similar to that used by Johnson [17] in the so-called elastic foundation model of the contact between a sphere and a layer on a rigid substrate. Expression (9) can therefore be viewed as extension of this approach to the case of a deformable substrate, where the oedometric nature of the layer is also fully accounted for.

Finally, it transpires that the response of a confined contact can be dissociated into two separate components as depicted in figure 1(b). The first one is the oedometric compression of the layer within the circular contact area of radius, $a$. The second contribution corresponds to the deformation of the substrate under the action of the surface stress applied over the same contact area of radius, $a$. The validity of this description is subsequently considered both from a comparison with exact contact mechanics calculation and experiments. Then a discussion is presented of its generalization to lateral deformation.

### 2.2. *Validation of the approximate indentation model*

#### 2.2.1. *Comparison to exact contact mechanics solutions*

Due to mixed boundary conditions, the Green function developed by Li and Chou [13] (equation (1)) for the contact of an axisymetric indenter to a coated substrate cannot be directly used to provide a solution in the real space. However, the use of auxiliary functions developed in [18,19] was shown by Perriot and Barthel [12] to allow the inversion of the contact problem at low numerical cost. Using this approach, contact forces were calculated as a function of the geometrical confinement of the contact, $a/t$. Similar calculations were also carried out after substitution of the exact expression for $X(\xi)$ (equation (2)) by its first order development corresponding to the oedometric approximation.

The results of these two separate calculations are shown in figure 2, where the non dimensional indentation load $\bar{P} = 3PR/4E_1^*a^3$ is reported as a function of $a/t$ for various ratios of the substrate to layer reduced modulii. In this calculation, the Poisson's ratio of the substrate was set to 0.2 and that of the layer to 0.4. From this figure, it turns out that the oedometric approximation allows for very accurate description of the indentation behaviour as long as the geometrical confinement of the contact, $a/t$, is greater than about 10.

On the other hand, an increased departure from the exact contact mechanics solution is systematically observed for low confinements. Whereas the exact model converges to the expected Hertzian response of the film (i.e. $\bar{P} \to 1$ when $a/t \to 0$), the approximate model shows a linear decrease of the non dimensional load with $a/t$ in the considered log–log plot, with a slope which is close to unity. This linear behaviour can easily be explained by considering that the substrate deformation becomes negligible as $a/t$ decreases. Accordingly, the oedometric approximation becomes equivalent in this regime to the contact of an elastic foundation on a rigid substrate, as detailed by Johnson [17]. In this model, the indentation load was found to obey the following relationship:

$$P = \frac{\pi}{4}\frac{\tilde{E}_1}{t}\frac{a^4}{R} \tag{10}$$

which can be rewritten in the following non dimensional form:

$$\bar{P} = \frac{\pi}{4}\frac{(1-\nu_1)^2}{(1-2\nu_1)}\frac{a}{t} \tag{11}$$

thus implying a linear dependence of $\log(\bar{P})$ with $\log(a/t)$ with a slope equal to unity, as it is observed in the case of our approximate model.

The insufficiencies of the oedometric description in the low confinement regime probably arise from the fact that it can no longer be assumed that the normal contact stresses within the layer do not expand outside the contact zone. They can therefore be considered as an indication of the limits of the geometrical confinement hypothesis embedded in the formulation of the approximate model.

The influence of the Poisson's ratio of the layer was further considered in a set of calculations carried out using $E_0^*/E_1^* = 50$. As the Poisson's ratio increases, a progressive departure of the approximate model from the exact contact mechanics solution is observed (figure 3). At high Poisson's ratio of the film (i.e. $\nu_1 > 0.4$), the oedometric approximation overestimates largely the indentation load over the whole $a/t$ range under consideration. This discrepancy with the exact contact mechanics solution can be considered as a consequence of the increased contribution of shear effects within the confined layer when it becomes close to incompressibility. As a result of these enhanced shear strains, the actual stiffness of the layer is probably decreased as compared to that corresponding to a purely oedometric compressive response. These limitations of the approximate model also clearly appear when the first order development of $X(\xi)$ is considered for high Poisson's ratios of the layer: the results reported in figure 4, show that the linear approximation of $X(\xi)$ in

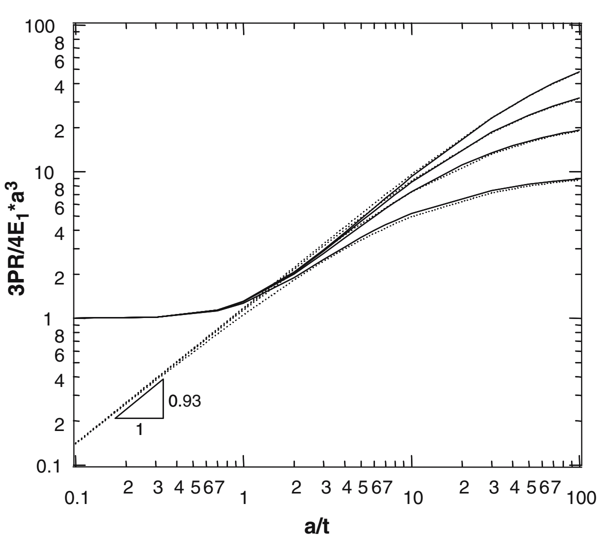


Figure 2. Non dimensional indentation load, $\bar{P} = 3PR/4E_1^*$, as a function of the ratio of the contact radius, $a$, to the layer thickness, $t$. These curves were calculated for increasing values of the substrate to coating reduced moduli ratio. From bottom to top $E_0^*/E_1^* = 10$; $E_0^*/E_1^* = 25$; $E_0^*/E_1^* = 50$; $E_0^*/E_1^* = 100$; $E_0^*/E_1^* = 200$. The dotted lines correspond to the oedometric approximation, the continuous lines to the exact contact mechanics solution derived by Perriot and Barthel [12] for coated contacts. ($\nu_0 = 0.2$; $\nu_1 = 0.4$).

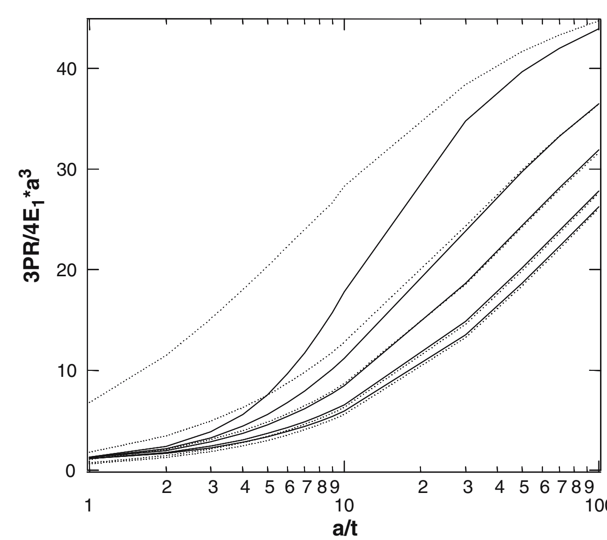


Figure 3. Non dimensional indentation load, $\bar{P} = 3PR/4E_1^*a^3$, as a function of the ratio of the contact radius, $a$, to the layer thickness, $t$. These curves were obtained for increasing values of the Poisson's ratio of the coating. From bottom to top: $\nu_1 = 0.2$; $\nu_1 = 0.3$; $\nu_1 = 0.4$; $\nu_1 = 0.45$; $\nu_1 = 0.49$. The dotted lines correspond to the oedometric approximation, the continuous lines to the exact contact mechanics solution derived by Perriot and Barthel [12] for coated contacts. ($\nu_0 = 0.2, E_0^*/E_1^* = 50$).

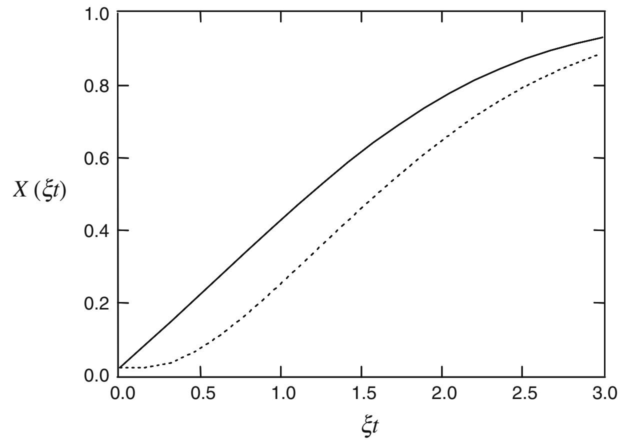


Figure 4. Plots of $X(\xi t)$ as a function of $\xi t$ for two different values of the Poisson's ratio of the layer, $\nu_1$. Continuous line: $\nu_1 = 0.3$; dotted line $\nu_1 = 0.5$. ($\nu_0 = 0.2, E_0^*/E_1^* = 50$).

the low $t$ regime is no longer valid at high Poisson's ratio.

In such a regime, it also transpires that the response of the layer will become increasingly sensitive to small variations of the Poisson's ratio as $\nu_1 \rightarrow 0.5$. Such problems have already been outlined in the context of numerical simulations of flat punch indentation of thin films on rigid substrates [20], where the contact compliance was found to depend strongly on the value of $\nu_1$ up to the 4st decimal close to 0.5. This sensitivity to the Poisson's ratio close to incompressibility strongly questions the accuracy of modulus measurements based on indentation experiments within confined systems, as $\nu_1$ is generally not known with the required precision [21]. These experimental limitations are potentially relevant to many polymer systems including gels, soft adhesives and polymer coatings in their glass transition or rubbery zone.

As a conclusion, this theoretical analysis of indentation loading indicates that the oedometric approximation is adequate for the analysis of confined films, provided that they are not to close to incompressibility. The validity of the oedometric approximation is further considered from the analysis of experimental indentation data using polymer films in their glassy range, which fulfil the condition $\upsilon_1 < 0.5$.

### 2.2.2. Analysis of experimental indentation data using glassy polymer films

Experimental indentation data have been obtained using macroscopic contacts with smooth glass lenses with centimetric radii of curvature ($R = 2$–$10$ cm). The tests have been carried out using glassy acrylate polymers films 18–79 $\mu$m in thickness, which were polymerized on thick glass substrates. A coupling agent (3-methacryloxy-propyl-dimethyl chlorosilane) was used in order to promote a good adhesion between the acrylate layer and the glass substrate. From a knowledge of the materials bulk elastic properties, the ratio $E_0^*/E_1^*$ was estimated to be about 50 for this system. The Poisson's ratio of the bulk polymer was found to be $\upsilon_1 = 0.4$ from tensile experiments. For each of the considered film thicknesses and radii of curvature, the radius of the contact was measured in the elastic range as a function of the applied normal load. For more details regarding the elaboration of the films and the experimental set-up, the reader is sent to reference [22].

When reported in a non dimensional plot giving $PR/a^3$ as a function of $a/t$, all the experimental data rescale onto a single relationship (figure 5). It was subsequently attempted to identify the oedometric modulus of the film from a least square fit using the experimental data and the approximate oedometric model. In this calculation, the reduced modulus of the substrate, $E_0^*$, was taken as the reduced modulus of the substrate/indenter system in order to account for the deformation of the glass sphere. The obtained oedometric modulus, $\tilde{E}_1 = 2800$ MPa, is very consistent with the value ($\tilde{E}_1 = 2500$ MPa) which is calculated using equation (4) and the bulk elastic constants ($E_1 = 1200$ MPa; $\nu_1 = 0.4$). This fitting of the experimental results by the approximate model gives an error of about 10%, which is not bad if one takes into account that these data were obtained using a wide range of film thicknesses (from 18 $\mu$m to 79 $\mu$m) and indenters geometries (radii of curvatures from 14 mm to 360 mm). The analysis of the experimental indentation data therefore confirms the essentially oedometric nature of the response of the studied glassy polymer film under confined contact conditions.

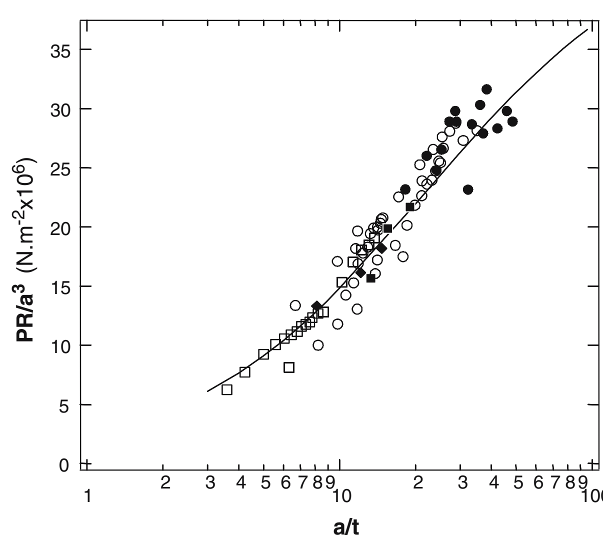


Figure 5. Experimental indentation data reported in a non dimensional plot giving the normalized indentation load, $PR/a^3$, as a function of the ratio of film thickness to contact radius, $a/t$. The data were obtained using glass lenses with radii of curvature varying between 14 mm and 360 mm. Film thicknesses: (●) 18 $\mu$m (○) 33 $\mu$m (■) 48 $\mu$m (□) 79 $\mu$m. The solid line correspond to the theoretical indentation response calculated using the oedometric approximation with $\tilde{E}_1 = 2800$ MPa.

## 3. Lateral contact loading

### 3.1. Approximate model for the lateral contact stiffness

To our best knowledge, no analytical model is available which can be used to derive first order approximations for the lateral contact loading of confined films. However, the above detailed theoretical analysis of the indentation of confined systems provides a description of the contact deformation behaviour, which can reasonably be extended to lateral contact loading situations. Within the context of this study, we were especially interested in the development of an approximate model relating the lateral contact stiffness to the shear modulus of the film. As for the normal indentation case, we assumed that the lateral load applied to the surface is integrally transmitted to the substrate over a constant contact area. As a result, the lateral contact stiffness can be dissociated into two separate components.

The first one corresponds to the shear response of the elastic film disk enclosed within the contact. As for normal contacts, the layer was assumed to behave as a set of elastic stiffnesses in parallel. However, this pure shear hypothesis implies that the relevant modulus for the layer is the shear modulus of the layer instead of its oedometric modulus. Contrary to normal indentation, no singularity is therefore expected in the lateral response when the film becomes close to incompressibility. Neglecting edge effects, the stiffness, $k_f$, of the film is simply given by:

$$k_f = \pi G_1 \frac{a^2}{t} \tag{12}$$

where $G_1$ is the shear modulus of the film.

The second component involved in the lateral response corresponds to the contact deformation of the substrate. The associated stiffness, $k_s$, is given by the classical Mindlin's theory [23]:

$$k_s = 8G_0^* a \tag{13}$$

where $G_0^*$ is the reduced shear modulus of the substrate defined by:

$$G_0^* = \frac{G_o}{2 - v_o} \tag{14}$$

The applied stress being transmitted integrally to the substrate over a constant contact area, the film and the substrate can be assumed to behave as stiffnesses in series [24], i.e.:

$$\frac{1}{k_c} = \frac{1}{k_f} + \frac{1}{k_s} \tag{15}$$

where $k_c$, is the contact stiffness of the coated system. Accordingly, the lateral stiffness of the coated contact can be expressed as:

$$k_c = \frac{8G_0^* a}{1 + \frac{8}{\pi}\frac{G_0^*}{G_1}\frac{t}{a}} \tag{16}$$

As mentioned above, the important point in equation (16) is that, as opposed to the normal indentation approximation, which involves a $1/(1\text{–}2v_1)$ term, this lateral model behaves smoothly with respect to all parameters.

### 3.2. Application to the measurement of the viscoelastic properties of confined polymer films

Lateral contact measurements have been carried out using a specific device, which is fully described in reference [22]. The experiments consisted in applying small amplitude lateral sinusoidal micro-motions to the coated contacts under a constant applied normal force. The displacement amplitude was kept in the submicrometric range in order to avoid any potential effects of micro-slip on the contact lateral response. As detailed in reference [22], this later hypothesis was validated by considering the linearity of the contact response. Within the investigated displacement domain, the magnitude of the tangential response was strictly proportional to the amplitude of the applied displacement, which would not be the case in the event of substantial micro-slip effects. Within the investigated linear regime, the contact behaviour can thus be assimilated to the drag of a circular region of the coated sample surface by the glass lens. Accordingly, one can therefore expect to be able to relate the measured complex contact stiffness, $k_c^*$, to the viscoelastic shear modulus using the approximate expression reported in equation (16).

Experiments have been carried out using films with different thicknesses and glass lenses with various radii of curvature. For each contact condition, the in-phase contact stiffness, $k_c'$, was measured at 3.2 Hz by Fast Fourier Transform [22]. All the results have been synthesised in figure 6, where the reduced in-phase contact compliance, $a/k_c'$, has been reported as a function of the ratios, $t/a$. All the results rescale onto a single linear plot in accordance with the following linearized formulation of the approximate model:

$$\frac{a}{k_c'} = \frac{1}{8G_0^*} + \frac{1}{\pi G_1'}\frac{t}{a} \tag{17}$$

where $G_1'$ is the storage (in-phase) modulus of the film. Accordingly, the intercept provided an estimate of the substrate reduced modulus and the slope a value of the storage shear modulus, $G_1' = 500 \pm 100$ MPa, which was consistent with the bulk value ($G_1 = 490$ MPa).

The shear modulus measurements were repeated as a function of temperature in order to determine the properties of the confined films in the glass transition

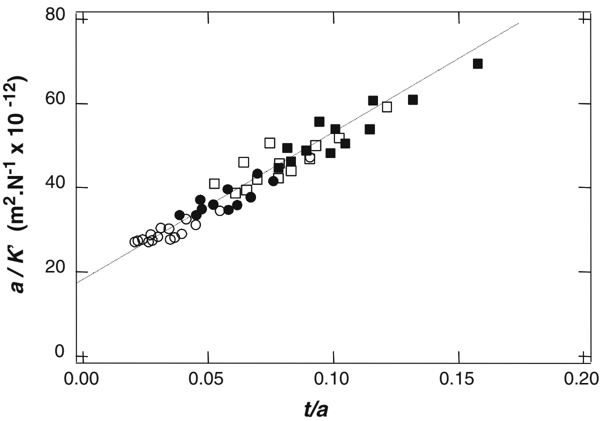


Figure 6. Reduced lateral contact compliance, $a/k_c'$, as a function of the ratio of the film thickness, $t$, to the contact radius, $a$. $k_c'$ is the in-phase contact stiffness measured at 3.2 Hz and 20 °C. The experiments have been carried out using glass lenses with radii varying between 20 and 100 mm. Film thicknesses: (■) 18 $\mu$m (□) 33 $\mu$m (○) 48 $\mu$m (●) 64 $\mu$m. According to the approximate contact model (equation (17)) a linear behaviour is observed. The slope provides an estimate of the storage shear modulus of the film.

zone. In addition to the storage modulus, the temperature dependence of the tangent of loss angle of the films, tan $\delta$, was also determined. The glass substrates being completely elastic over the considered temperature range, a measurement of the phase shift should directly provide an estimate of the loss tangent of the film, independently of any contact model. When using such an approach, one has to take care, however, of potential artifacts, which can arise as a result of the mechanical coupling of the viscoelastic and elastic parts of the system. For metal/polymer/metal assemblies, such effects have been reported to induce some unexpected shift of the loss factor peak as a function of specimen geometry or film thickness [25]. A simple first order calculation using our approximate contact model showed, however, that such effects are not expected to be significant during the considered lateral contact measurements.

In figure 7, the measured film viscoelastic properties have been reported as a function of temperature for different applied normal loads. Preliminary Differential Scanning Calorimetry (D.S.C.) measurements indicated that the glass transition of the films was 52 °C at 10 °C/min and the contact experiments were thus carried out in the temperature range 20–100 °C. As a reference, the previously reported [22] viscoelastic response of an unconfined contact with a bulk acrylate has also been reported in the figure.

As expected, a strong drop in G′ and a damping peak were systematically observed in the glass transition zone. The interesting point is, however, that increasing applied contact loads induce a significant shift of the glass transition zone to higher temperatures. Depending on the applied load, it appears that the glass transition temperature of the confined films can be shifted by more than 20 °C. Such an effect can tentatively be explained by the essentially hydrostatic nature of the contact pressure applied to the confined films. Relaxations in polymers are known to involve segmental motions, which require a certain amount of available volume, or ‘free volume’, within the bulk polymers. Consequently, the application of a hydrostatic pressure is expected to hinder these movements; this in turn implies that the mechanical relaxation should occur at an increased temperature. Data reviewed by Parry and Tabor [26] indicate that such effects were effectively reported for both semi-crystalline and glassy polymers. For bulk acrylate materials such as Poly(methylmethacrylate), available data indicates that the shift in the glass transition caused by hydrostatic pressure is approximately 0.2–0.3 °C/$10^6$ Pa [26,27]. These data are consistent with the observed shift of the glass

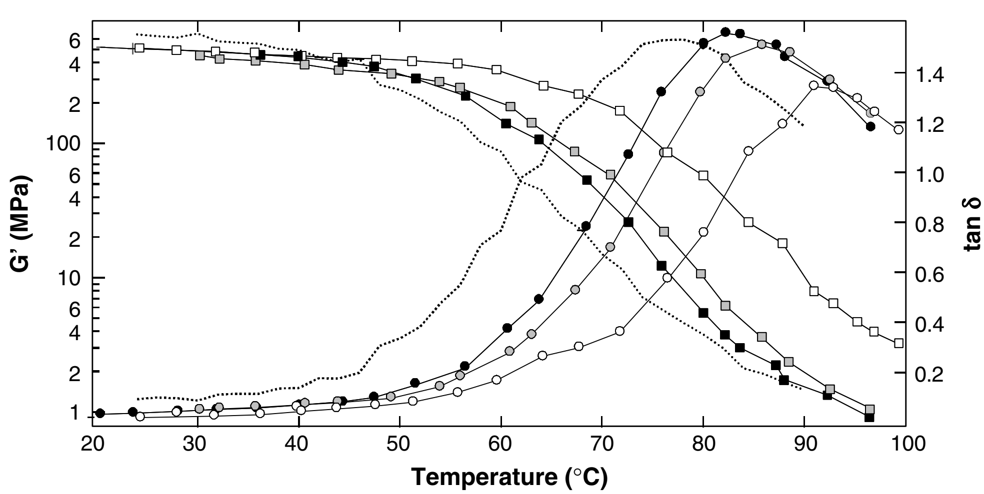


Figure 7. Storage modulus, $G'$, and tangent of the loss angle, tan $\delta$, of confined polymer films determined from lateral contact stiffness measurements. Circles: tan $\delta$, squares : G′. The tests have been carried out at increasing applied normal loads. Black symbols: $P = 40$ N; grey symbols : $P = 100$ N; open symbols : $P = 240$ N;. (frequency = 3.2 Hz, film thickness = 33 $\mu$m). The dotted lines correspond to the values of $G'$ and tan $\delta$ measured by the same contact method using a bulk acrylate specimen, i.e. under unconfined conditions (data taken from reference [22]).

temperature transition in our contact experiments (0.3 °C/$10^6$ Pa), which can be viewed as an indirect confirmation of the essentially hydrostatic nature of the contact pressure.

## 4. Conclusion

In this study, a first order approximation of an analytical contact model was developed in order to get some insight into the behaviour of confined films. This approach allowed drawing a simple picture of the contact response under normal indentation loading. It was found that the film response is of an essentially oedometric nature while the deflection of the elastic substrate is dictated by the applied normal stress. This simplified description of confined contacts fails, however, in the case of coatings close to incompressibility as a result of the complex interplay between compression and shear deformations within the confined layers. Moreover, exact contact mechanics simulations in this regime show that the contact response becomes increasingly sensitive to small uncertainties in the value of the Poisson's ratio of the layer. From these considerations, it comes out that indentation loading is probably not the most appropriate configuration to assess the mechanical properties of films close to incompressibility when confinement effects come into play. Such an issue is relevant to many practical situations involving soft polymers films in their glass transition zone or rubbery region.

On the other hand, a similar analysis of the shear behaviour of confined films shows that such difficulties are not expected under lateral contact measurements. This point was confirmed by experiments carried out using crosslinked acrylate films, which provided consistent values of the shear viscoelastic moduli in the glass transition zone. Using this approach, the strong sensitivity of the glass transition of polymer coating to hydrostatic pressure was established. As a consequence, it is shown that the thermo-mechanical properties of polymer coatings confined within contacts can be largely different from their bulk values. Such an observation is especially relevant to tribological situations involving polymer coatings with some potential implications regarding the friction and wear processes.

## Acknowledgments

Hélène Montes is thanked for her help in the preparation and the characterisation of the samples as well as for many fruitful discussions. We also thank François Lequeux for helpful discussion about film confinement effects.

## References

[1] G.M. Pharr, W.C. Oliver and F.R. Brotzen, J. Materials Res. 7(3) (1992) 613.
[2] J. Mencick, D. Munz, E. Quandt and E.R. Weppelman, J. Materials Res. 12(9) (1997) 2475.
[3] M.F. Doerner and W.D. Nix, J. Materials Res. 1(4) (1997) 601.
[4] R.B. King, Int. J. Solids Structures 23(12) (1987) 1657.
[5] R. Saha and W.D. Nix, Acta Materialia 50(1) (2002) 23.
[6] S. Bec, A. Tonck, J.M. Georges, E. Georges and J.L. Loubet, Philos. Magazine 74(5) (1996) 1061.
[7] H. Gao, C.H. Chiu and J. Lee, Int. J. Solids Structures 29(20) (1992) 2471.
[8] A. Strojny, X.Y. Xia, A. Tsou and W.W. Gerberich, J. Adhesion Sci. Technol. 12(12) (1998) 1299.
[9] S. Roche, S. Pavan, J.L. Loubet, P. Barbeau and B. Magny, Prog. Organic Coatings 47(1) (2003) 37.
[10] J.A. Payne, A. Strojny, L.F. Francis and W.W. Gerberich, Polymer Eng. Sci. 38(9) (1998) 1529.
[11] D.E. Kramer, A.A. Volinsky, N.R. Moody and W.W. Gerberich, J. Materials Res. 16(11) (2001) 3150.
[12] A. Perriot and E. Barthel, J. Materials Res. 19(2) (2004) 600.
[13] J. Li and T.-W. Chou, Int. J. Solids Structures 34(35–36) (1997) 4463.
[14] T. Nogi and T. Kato, ASME J. Tribol. 119 (1997) 493.
[15] Y.Y. Lin, C.-Y. Hui and H.D. Conway, J. Polymer Sci. Part B Polymer Phy. 38(21) (2000) 2769.
[16] Landau, L.D. and Lifshitz, E.M., *Theory of elasticity*. (Pergamon, 1986).
[17] K.L. Johnson, *Contact Mechanics* (Cambridge University Press, Cambridge, 1985).
[18] A.S. Huguet and E. Barthel, J. Adhesion 74(1–4) (2000) 143.
[19] E. Barthel and G. Haiat, Langmuir 18(24) (2002) 9362.
[20] J.F. Ganghoffer and A.N. Gent, J. Adhesion 48 (1995) 75.
[21] N.W. Tschoegl, W.G. Knauss and I. Emri, Mechanics Time-Dependent Materials 6(1) (2002) 3.
[22] E. Gacoin, A. Chateauminois and C. Fretigny, Polymer 45 (2004) 3789.
[23] R.D. Mindlin, ASME Trans., J. Appl. Mechanics, Series E 16 (1953) 327.
[24] A. Tonck, J. Sabot and J.M. Georges, J. Tribol. 106 (1984) 35.
[25] P. Cuillery, R. Gaertner, J. Tatibouet and M. Mantel, J. Appl. Polymer Sci. 65 (1997) 2493.
[26] E.J. Parry and D. Tabor, J. Materials Sci. 8 (1973) 1510.
[27] E.J. Parry and D. Tabor, J. Materials Sci. 9 (1974) 289.